show ice concentration increases (Plate 2a), the ice-free areas within the ice pack also increased (Table 3), a result, in this case, of the increased ice extent (Table 1) and hence the larger area over which the ice-free areas within the ice pack were summed.

In spring the largest-magnitude ice concentration trends are the negative trends in the eastern Barents Sea (Plate 2b), where they are also statistically significant (Plate 3b). These negative trends coincide with decreases in ice extent, ice area, and ice-free area within the ice pack (Tables 1-3), indicating a much reduced ice cover. In summer the largest-magnitude trends are the negative trends in the East Siberian Sea (70-76°N, 155-175°E) and in smaller areas north of Asia and the positive trends off the west coast of Greenland in northeastern Baffin Bay and in the eastern Beaufort Sea at about 130°W and 72°N (Plate 2c). In each of these cases the corresponding regions of section 3 are too large for ready comparisons, although, in general, there is a high significance level, with a ratio of trend to estimated standard deviation exceeding 3 (Plate 3c). In autumn also, the East Siberian Sea has negative ice concentration trends, northeastern Baffin Bay has positive ice concentration trends, and the eastern Beaufort Sea has positive ice concentration trends (Plate 2d), but in each of these cases the magnitude is reduced from that of the summer trends (Plate 2c). In autumn the highest-magnitude trends are the negative trends in the southern Kara Sea and off the coast of northern Alaska at about 165°W (Plate 2d). Once again, the highest-magnitude trend values exceed 3 estimated standard deviations (Plate 3d).

6. Discussion

As shown in section 3 and by *Cavalieri et al.* [1997], monthly averaged passive-microwave data from the SMMR and SSMI instruments over the period November 1978 through December 1996 reveal an overall negative trend in ice extents for the Northern Hemisphere. This result agrees with results previously found by *Johannessen et al.* [1995] and *Bjørgo et al.* [1997] for slightly shorter periods. As also shown in section 3, the negative trend comes regionally mostly from the Kara and Barents Seas and the next two major regional contributors to the negative slope are the Seas of Okhotsk and Japan and the Arctic Ocean. Lesser contributions come from the Greenland Sea, Hudson Bay, and the Canadian Archipelago (Table 1). The remaining three regions, the Bering Sea, Baffin Bay/Labrador Sea, and the Gulf of St. Lawrence, exhibit slight, positive trends over the SMMR/SSMI period, with the largest positive trend being for the region of Baffin Bay/Labrador Sea but the only statistically significant positive trend (at a 95% confidence level or above) being for the Gulf of St. Lawrence (Table 1).

For most regions and the total, changes from one year to another often far exceed the rate of change indicated in the long-term trend, and adjustment by a few years of the starting and/or ending times of the trend calculation would, in some instances, change the sign of the slope. Hence we caution against extrapolating the trend lines and slopes given here to times prior to the November 1978 start of the data set or subsequent to the December 1996 end of the data set. The results presented provide specific, quantified information about Arctic sea ice extents over an 18.2-year period, showing considerable regional and interannual variability but no trends that can be clearly identified as long-term climate trends appropriate for extrapolation beyond the 18.2 years. In fact, an analysis of Arctic sea ice fluctuations over the 25 years 1953-1977, prior to the SMMR/SSMI time period, reveals a slight (3140 km^2/yr) but statistically significant positive trend in 1953-1977 ice extents [*Walsh and Johnson*, 1979]. The negative trend (-34,000 km^2/yr) reported here for the yearly averages in the Northern Hemisphere as a whole over the 18-year period 1979-1996 is an order of magnitude greater than the 1953-1977 positive trend but is for a shorter period.

To confirm that the ice extent trends of Figures 1-10 and Table 1 are robust in terms of not being dramatically dependent on the choice of 15% as the ice concentration cutoff used in the definition of ice extent, the calculations were redone using 20% and then 30% as the ice concentration cutoff. (For instance, in the 20% case, ice extent is defined as the cumulative area of all grid cells, in the region of interest, having calculated sea ice concentrations of at least 20%.) Figure 14 presents the yearly average results for each region having statistical significance in the yearly averaged trend (Table 1) and additionally the seasonal results for the Northern Hemisphere totals. This selection is a good sampling of the results for all of the regions and seasons, showing the near but not perfect parallelism of the 15%, 20%, and 30% curves. In each case the sign of the slope of the line of linear least squares fit is the same, irrespective of which ice concentration cutoff is used; and although the magnitudes of the slopes are generally different for the different cutoffs, in each case the level of statistical significance (95%, 99%, or none) remains the same (Table 4). Furthermore, in all cases except one, the slopes of the 20% and 30% ice extents are within 1 standard deviation of the 15% ice extent slope.

The smaller percent interannual variability in the Northern Hemisphere total than in many of the regions (Figure 1a versus the regional monthly average plots) reflects the compensating changes that often occur, many times as a result of atmospheric pressure systems that tend to lessen ice coverage in one region while increasing it in another. Examples include the occasional out-of-phase nature of the ice coverages of the Bering Sea and the Sea of Okhotsk [*Cavalieri and Parkinson*, 1987] and of other pairs of adjacent seas separated by a geographical boundary. The particularly strong interannual variability found in the ice extents of the Greenland Sea and the Kara and Barents Seas (Figures 7a and 8a) is likely related to the influence of North Atlantic storm systems. In fact, the strongest winter cyclones in the north polar region tend to be over the Iceland and Norwegian Seas, with the highest cyclone frequencies being just south of Iceland and high frequencies also occurring between Svalbard and Scandinavia and over the Norwegian and Kara Seas [*Serreze et al.*, 1993]. Central cyclonic pressures in these regions are frequently below 970 mbar [*Serreze et al.*, 1993], generating winds that will, depending upon the precise positioning of the cyclone, sometimes decrease ice extents in the Greenland Sea by pushing the ice toward the Greenland coast and other times increase ice extents in the Greenland Sea by spreading ice southward. Similarly, they will sometimes decrease and sometimes increase the ice coverage in the Kara and Barents Seas. *Shuchman et al.* [1998] provide more details specifically for the Odden feature in the Greenland Sea ice cover, showing, through comparisons between ice and atmospheric data, the importance of temperature and wind conditions to the Odden growth, maintenance, and decay.

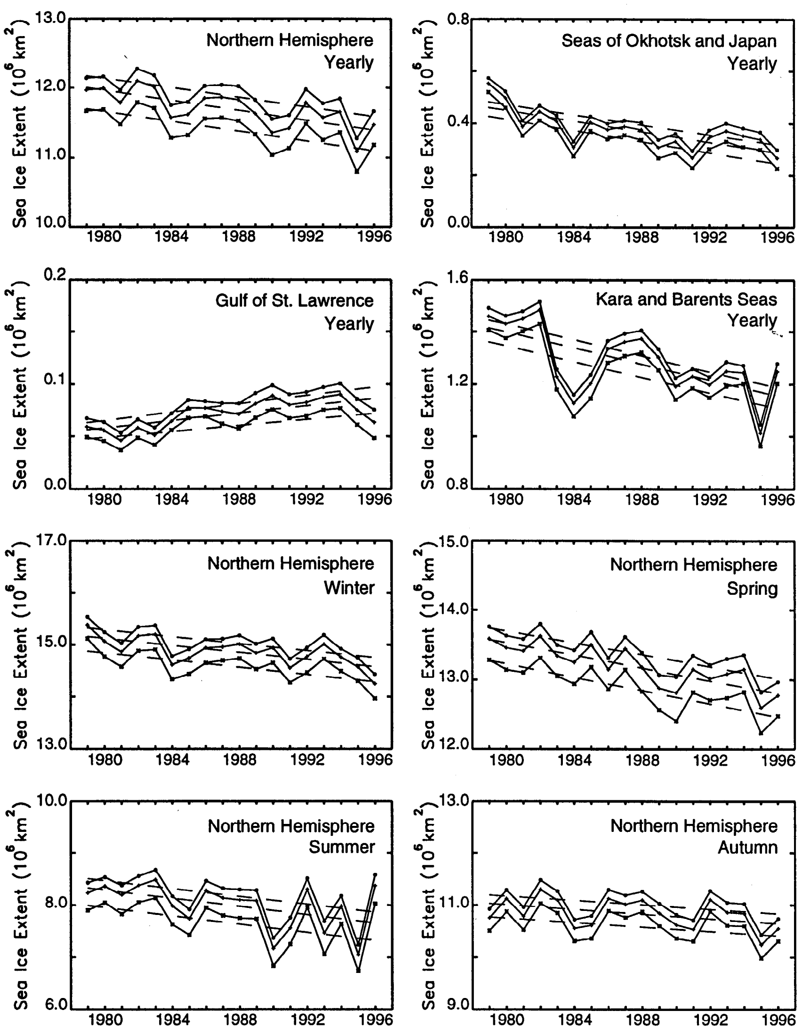

Figure 14. Selection of yearly and seasonal ice extent values and trend lines plotted for three choices of ice concentration cutoff used in the definition of ice extent. In each case the top curve uses a 15% ice concentration cutoff, as in Figures 1-10, whereas the middle curve uses a 20% cutoff and the bottom curve uses a 30% cutoff. Yearly values are plotted for the Northern Hemisphere, the Seas of Okhotsk and Japan, the Gulf of St. Lawrence, and the Kara and Barents Seas; and seasonal values are plotted for the Northern Hemisphere.

Table 4. Slopes, and Their Estimated Standard Deviations, of the Lines of Linear Least Squares Fit Through 1979-1996 Yearly Sea Ice Extents for Regions With Statistically Significant Yearly Slopes in Table 1 and Seasonal Sea Ice Extents for the Northern Hemisphere

Region	Type	15% Cutoff		20% Cutoff		30% Cutoff	
		10^3 km^2/yr	S	10^3 km^2/yr	S	10^3 km^2/yr	S
Northern Hemisphere	yearly	-34.0 ± 8.3	99	-35.6 ± 8.4	99	-35.8 ± 8.4	99
Seas of Okhotsk and Japan	yearly	-9.7 ± 2.3	99	-10.3 ± 2.3	99	-10.8 ± 2.3	99
Gulf of St. Lawrence	yearly	2.0 ± 0.4	99	1.8 ± 0.4	99	1.4 ± 0.5	99
Kara and Barents Seas	yearly	-15.2 ± 4.4	99	-15.2 ± 4.5	99	-14.9 ± 4.5	99
Northern Hemisphere	winter	-33.6 ± 9.2	99	-34.3 ± 9.2	99	-34.0 ± 9.2	99
Northern Hemisphere	spring	-42.8 ± 7.5	99	-45.5 ± 7.7	99	-47.6 ± 8.1	99
Northern Hemisphere	summer	-38.3 ± 17.6	95	-40.0 ± 17.5	95	-40.0 ± 17.3	95
Northern Hemisphere	autumn	-21.5 ± 11.9		-22.7 ± 12.0		-21.7 ± 12.2	

Slopes are provided for three choices (15%, 20%, and 30%) of ice concentration cutoff in the definition of ice extent. S indicates statistical significance and identifies those cases in which the null hypothesis of a 0 slope is rejected with a 95% confidence level (95) and a 99% confidence level (99), using a standard *F* test with 16 degrees of freedom.

The ice increases in Baffin Bay/Labrador Sea and the Gulf of St. Lawrence (Figures 5-6) contrasted with the decreases in the Greenland Sea, Kara and Barents Seas, and Arctic Ocean (Figures 7-9) are likely tied to the large-scale atmospheric patterns of the North Atlantic Oscillation. The NAO, calculated as the normalized atmospheric pressure at Lisbon, Portugal, minus that at Stykkisholmur, Iceland, has been above average since 1980, with a strong Azores High and, most importantly for the sea ice cover, a strong Icelandic Low [*Hurrell*, 1995; *Dickson et al.*, 1996]. The result includes strong southwesterlies across the North Atlantic, with anomalously high temperatures over northern Europe and Asia, and strong north winds over Baffin Bay and the Labrador Sea, with consequent anomalously low temperatures in those regions [*Hurrell*, 1995; *Hurrell and van Loon*, 1997]. In addition to an intensified Icelandic Low, atmospheric pressures have also decreased over the Arctic Ocean, as revealed from data of the Arctic Ocean Buoy Program for 1979-1994 [*Walsh et al.*, 1996]. This has decreased the anticyclonic wind forcing on the Arctic Ocean sea ice and decreased the atmospheric forcing of the Transpolar Drift Stream across the Arctic Basin, through Fram Strait, and into the Greenland Sea [*Walsh et al.*, 1996]. Decreased southward flow into the Greenland Sea is consistent with the decreasing sea ice extents found for the Greenland Sea (Figure 7, Table 1). The sea ice trends determined for these regions from the 1978-1996 SMMR and SSMI data (Figures 5-9, Table 1) can thus be viewed as a part of the larger-scale happenings within the climate system, in this case particularly the NAO in atmospheric pressures between Iceland and Portugal and the decreases in Arctic atmospheric pressures. The NAO influence also extends well below the ocean surface, with the rise in the NAO index since the 1960s being believed to have contributed to the decreasing deep convection in the Greenland Sea and the increasing deep convection in the Labrador Sea [*Dickson et al.*, 1996]. This, in turn, has led to warming of the deep water of the Greenland Sea and cooling of the deep water of the Labrador Sea [*Dickson et al.*, 1996].

On longer timescales many studies have found an expected negative correlation between sea ice coverage and atmospheric temperatures. For instance, such correlations were found by *Rogers* [1978] in the Beaufort Sea, by *Walsh and Johnson* [1979] for the Arctic as a whole, and by *Manak and Mysak* [1989] for the Beaufort Sea, Hudson Bay, and Baffin Bay/Labrador Sea. Using a 30-year record from 1961 to 1990, *Chapman and Walsh* [1993] found Arctic sea ice variations to be consistent with the corresponding air temperature changes, the latter showing an overall warming in the Arctic, although a cooling over Baffin Bay, the Labrador Sea, and the southern Greenland Sea (conducive to ice extent decreases in the Arctic and increases in Baffin Bay/Labrador Sea, as in Figures 5 and 9 and Table 1). Seasonally, the 1961-1990 warming was strongest in winter and spring, whereas the sea ice decreases were highest in spring and summer [*Chapman and Walsh*, 1993]. (Relatedly, the Intergovernmental Panel on Climate Change (IPCC) found warming from 1955-1974 to 1975-1994 over much of the Arctic periphery but cooling over Baffin Bay, the Labrador Sea, and the southern Greenland Sea [*Nicholls et al.*, 1996]. However, in a separate study an overall warming was not detectable in the lower troposphere over the Arctic Ocean over the period 1950-1990 [*Kahl et al.*, 1993]. Temperature data for the Arctic have been notoriously sparse, although improved data sets from 1979 onward are now being generated through combining buoy data from the International Arctic Buoy Program with ship reports and data from drifting ice stations and coastal weather stations [*Martin and Munoz*, 1997].) Looking more specifically at anomalous years, *Mysak et al.* [1996] find unusually heavy ice coverages in Hudson Bay, Baffin Bay, and the Labrador Sea in each of the three periods, 1972/1973, 1982/1983, and 1991/1992, with simultaneous strong North Atlantic Oscillation and El Niño-Southern Oscillation episodes, in each case finding a link with low surface air temperature anomalies lasting for several seasons. The heavy ice coverages are consistent with the finding by *Mysak* [1986] of low sea surface temperatures in the northwest North Atlantic during El Niño episodes. These specific cases show connections between the ice cover and other elements of the climate system. As the records lengthen, the connections should be further clarified and the climate system more fully understood.

Acknowledgments. We gratefully acknowledge Jamila Saleh of Raytheon STX for her help in the generation of the figures; Jamila and her colleagues Steve Fiegles and Mike Martino, also of Raytheon STX, for the processing of the data; and the National Snow and Ice Data Center (NSIDC) in Boulder, Colorado, for providing the SSMI radiances. We also thank two anonymous reviewers and JGR editors Ruth Preller and Mark Drinkwater for their time and effort and Leif Toudal Pedersen and John Walsh for excellent reviews and suggestions. This work was supported by NASA's Earth Observing System (EOS) program and by the Polar Programs at NASA Headquarters.

References

Aagaard, K., and E. C. Carmack, The role of sea ice and other fresh water in the Arctic circulation, *J. Geophys. Res.*, *94*(C10), 14,485-14,498, 1989.

Barry, R. G., M. C. Serreze, J. A. Maslanik, and R. H. Preller, The Arctic sea ice-climate system: Observations and modeling, *Rev. Geophys.*, *31*(4), 397-422, 1993.

Bjørgo, E., O. M. Johannessen, and M. W. Miles, Analysis of merged SMMR-SSMI time series of Arctic and Antarctic sea ice parameters 1978-1995, *Geophys. Res. Lett.*, *24*(4), 413-416, 1997.

Cavalieri, D. J., and C. L. Parkinson, On the relationship between atmospheric circulation and the fluctuations in the sea ice extents of the Bering and Okhotsk Seas, *J. Geophys. Res.*, *92*(C7), 7141-7162, 1987.

Cavalieri, D. J., P. Gloersen, C. L. Parkinson, J. C. Comiso, and H. J. Zwally, Observed hemispheric asymmetry in global sea ice changes, *Science*, *278*, 1104-1106, 1997.

Cavalieri, D. J., C. L. Parkinson, P. Gloersen, J. C. Comiso, and H. J. Zwally, Deriving long-term time series of sea ice cover from satellite passive-microwave multisensor data sets, *J. Geophys. Res.*, *104*, 15,803- 15,814, 1999.

Chapman, W. L., and J. E. Walsh, Recent variations of sea ice and air temperature in high latitudes, *Bull. Am. Meteorol. Soc.*, *74*(1), 33-47, 1993.

Comiso, J. C., and R. Kwok, Surface and radiative characteristics of the summer Arctic sea ice cover from multisensor satellite observations, *J. Geophys. Res.*, *101*(C12), 28,397-28,416, 1996.

Dickson, R., J. Lazier, J. Meincke, P. Rhines, and J. Swift, Long-term coordinated changes in the convective activity of the North Atlantic, *Prog. Oceanogr.*, *38*(3), 241-295, 1996.

Draper, N. R., and H. Smith, *Applied Regression Analysis*, 2nd ed., 709 pp., John Wiley, New York, 1981.

Gloersen, P., and W. J. Campbell, Recent variations in Arctic and Antarctic sea-ice covers, *Nature*, *352*, 33-36, 1991.

Gloersen, P., W. J. Campbell, D. J. Cavalieri, J. C. Comiso, C. L. Parkinson, and H. J. Zwally, Arctic and antarctic sea ice, 1978-1987: Satellite passive-microwave observations and analysis, *NASA SP-511*, 290 pp., 1992.

Gloersen, P., J. Yu, and E. Mollo-Christensen, Oscillatory behavior in Arctic sea ice concentrations, *J. Geophys. Res.*, *101*(C3), 6641-6650, 1996.

Gloersen, P., C. L. Parkinson, D. J. Cavalieri, J. C. Comiso, and H. J. Zwally, Spatial distribution of trends and seasonality in the hemispheric sea ice covers: 1978-1996, *J. Geophys. Res.*, this issue.

Häkkinen, S., An Arctic source for the Great Salinity Anomaly: A simulation for the Arctic ice-ocean system for 1955-1975, *J. Geophys. Res.*, *98*(C9), 16,397-16,410, 1993.

Hurrell, J. W., Decadal trends in the North Atlantic Oscillation: Regional temperatures and precipitation, *Science*, *269*, 676-679, 1995.

Hurrell, J. W., and H. van Loon, Decadal variations in climate associated with the North Atlantic Oscillation, *Clim. Change*, *36*(3), 301-326, 1997.

Johannessen, O. M., M. Miles, and E. Bjørgo, The Arctic's shrinking sea ice, *Nature*, *376*, 126-127, 1995.

Kahl, J. D., D. J. Charlevoix, N. A. Zaitseva, R. C. Schnell, and M. C. Serreze, Absence of evidence for greenhouse warming over the Arctic Ocean in the past 40 years, *Nature*, *361*, 335-337, 1993.

Manak, D. K., and L. A. Mysak, On the relationship between Arctic sea-ice anomalies and fluctuations in Northern Canadian air temperature and river discharge, *Atmos.-Ocean*, *27*(4), 682-691, 1989.

Martin, S., and E. A. Munoz, Properties of the Arctic 2-meter air temperature field for 1979 to the present derived from a new gridded dataset, *J. Clim.*, *10*, 1428-1440, 1997.

Maslanik, J. A., M. C. Serreze, and R. G. Barry, Recent decreases in Arctic summer ice cover and linkages to atmospheric circulation anomalies, *Geophys. Res. Lett.*, *23*(13), 1677-1680, 1996.

Massom, R., *Satellite Remote Sensing of Polar Regions*, 307 pp., Belhaven, London, 1991.

Mysak, L. A., El Niño, interannual variability and fisheries in the northeast Pacific Ocean, *Can. J. Fish. Aquat. Sci.*, *43*, 464-497, 1986.

Mysak, L. A., and S. B. Power, Sea-ice anomalies in the western Arctic and Greenland-Iceland Sea and their relation to an interdecadal climate cycle, *Climatol. Bull.*, *26*, 147-176, 1992.

Mysak, L. A., R. G. Ingram, J. Wang, and A. van der Baaren, The anomalous sea-ice extent in Hudson Bay, Baffin Bay and the Labrador Sea during three simultaneous NAO and ENSO episodes, *Atmos. Ocean*, *34*(2), 313-343, 1996.

National Snow and Ice Data Center (NSIDC), DMSP SSM/I brightness temperatures and sea ice concentration grids for the polar regions on CD-ROM user's guide, *Spec. Rep. 1*, Coop. Inst. for Res. in Environ. Sci., Univ. of Colo., Boulder, 1992.

Nicholls, N., G. V. Gruza, J. Jouzel, T. R. Karl, L. A. Ogallo, and D. E. Parker, Observed climate variability and change, in *Climate Change 1995: The Science of Climate Change*, edited by J. T. Houghton et al., pp.133-192, Cambridge Univ. Press, New York, 1996.

Parkinson, C. L., The impact of the Siberian High and Aleutian Low on the sea-ice cover of the Sea of Okhotsk, *Ann. Glaciol.*, *14*, 226-229, 1990.

Parkinson, C. L., Recent sea-ice advances in Baffin Bay/Davis Strait and retreats in the Bellingshausen Sea, *Ann. Glaciol.*, *21*, 348-352, 1995.

Parkinson, C. L., and D. J. Cavalieri, Arctic sea ice 1973-1987: Seasonal, regional, and interannual variability, *J. Geophys. Res.*, *94*(C10), 14,499-14,523, 1989.

Parkinson, C. L., J. C. Comiso, H. J. Zwally, D. J. Cavalieri, P. Gloersen, and W. J. Campbell, Arctic sea ice, 1973-1976: Satellite passive-microwave observations, *NASA SP-489*, 296 pp., 1987.

Pollard, J. H., *A Handbook of Numerical and Statistical Techniques*, 349 pp., Cambridge Univ. Press, New York, 1981.

Pritchard, R. S. (Ed.), *Sea Ice Processes and Models*, 474 pp., Univ. of Wash. Press, Seattle, 1980.

Robinson, D. A., K. F. Dewey, and R. R. Heim, Global snow cover monitoring: An update, *Bull. Am. Meteorol. Soc.*, *74*(9), 1689-1696, 1993.

Rogers, J. C., Meteorological factors affecting the interannual variability of summertime ice extent in the Beaufort Sea, *Mon. Weather Rev.*, *106*, 890-897, 1978.

Serreze, M. C., J. E. Box, R. G. Barry, and J. E. Walsh, Characteristics of Arctic synoptic activity, 1952-1989, *Meteorol. Atmos. Phys.*, *51*, 147-164, 1993.

Serreze, M. C., J. A. Maslanik, J. R. Key, and R. F. Kokaly, Diagnosis of the record minimum in Arctic sea ice area during 1990 and associated snow cover extremes, *Geophys. Res. Lett.*, *22*(16), 2183-2186, 1995.

Shuchman, R. A., E. G. Josberger, C. A. Russel, K. W. Fischer, O. M. Johannessen, J. Johannessen, and P. Gloersen, Greenland Sea Odden sea ice feature: Intra-annual and interannual variability, *J. Geophys. Res.*, *103*(C6), 12,709-12,724, 1998.

Taylor, J. R., *An Introduction to Error Analysis: The Study of Uncertainties in Physical Measurements*, 2nd ed., 327 pp., Univ. Sci. Books, Sausalito, Calif., 1997.

Toudal Pedersen, L., D. Low, H. Valeur, and P. Wadhams, Satellite observations of the Odden ice cover during the winter of 1995-1996, *Rep. DTU R 656*, 46 pp., Tech. Univ. of Denmark, Lyngby, 1997.

Wadhams, P., N. R. Davis, J. C. Comiso, R. Kutz, J. Crawford, G. Jackson, W. Krabill, C. B. Sear, R. Swift, and W. B. Tucker III, Concurrent remote sensing of Arctic sea ice from submarine and aircraft, *Int. J. Remote Sens.*, *12*(9), 1829-1840, 1991.

Walsh, J. E., and C. M. Johnson, An analysis of Arctic sea ice fluctuations, 1953-77, *J. Phys. Oceanogr.*, *9*(3), 580-591, 1979.

Walsh, J. E., W. L. Chapman, and T. L. Shy, Recent decrease of sea level pressure in the Central Arctic, *J. Clim.*, *9*, 480-486, 1996.

D. J. Cavalieri, J. C. Comiso, P. Gloersen, C. L. Parkinson, and H. J. Zwally, Oceans and Ice Branch, Code 971, NASA Goddard Space Flight Center, Greenbelt, MD 20771. (Claire.L.Parkinson.1@gsfc.nasa.gov)

(Received June 15, 1998; revised January 22, 1999; accepted March 12, 1999.)